

A deep learning approach for Magnetic Resonance Fingerprinting

Mohammad Golbabae¹, Dongdong Chen², Pedro A. Gómez^{3,4}, Marion I. Menzel⁴ and Mike E. Davies².

¹Computer Science Department, University of Bath, ²School of Engineering, University of Edinburgh.

³Munich School of Bioengineering, Technische Universität München. ⁴GE Healthcare, Munich.

Abstract— Current popular methods for Magnetic Resonance Fingerprint (MRF) recovery are bottlenecked by the heavy storage and computation requirements of a matched-filtering step due to the growing size and complexity of the fingerprint dictionaries in multi-parametric quantitative MRI applications. In this abstract we investigate and evaluate advantages of a deep learning approach for embedding the manifold of solutions of the Bloch equations and to address these shortcomings.

1 Introduction

Magnetic Resonance Fingerprinting (MRF) recently emerged to accelerate acquisition of the *quantitative* NMR characteristics such as the T1, T2 and T2* relaxation times, field inhomogeneity, perfusion and diffusion [1, 2, 3, 4, 5]. As opposed to mainstream qualitative assessments these *absolute* physical quantities can be used for tissue or pathology identification independent of the scanner or scanning sequences. Unlike conventional quantitative approaches MRF uses i) short and often complicated excitation pulses which encode many NMR parameters simultaneously, and ii) significantly undersampled k-space data. To overcome the lack of sufficient spatio-temporal information MRF incorporates a physical model based on exhaustively simulating a large dictionary of magnetic responses (fingerprints) for all combinations of the quantized NMR parameters. This dictionary is then used for matched-filtering in a model-based reconstruction scheme e.g. [6]. As occurs to any multi-parametric manifold enumeration, the main drawback of such approach is the size of this dictionary which grows exponentially in terms of the number of parameters and their quantization resolution; a serious (non-scalability) limitation of the current methods to be applicable in the emerging multi-parametric MRF applications.

In this study we propose a dictionary-free deep learning approach to address this shortcoming. The proposed MRF-Net provides an efficient embedding for the *manifold* of solutions to the Bloch differential equation parametrized by the NMR characteristics. Our *in-vivo* experiment for estimating two parameters (i.e. a small-size MRF problem) indicates that the MRF-Net is able to achieve a good accuracy however with 3x less storage and model-fitting computations as required for a baseline dimension-reduced dictionary matching scheme (Figure 1).

2 Problem statement

MRF acquisitions follow a linear spatio-temporal model:

$$Y \approx \mathcal{A}(X), \quad (1)$$

where $Y \in \mathbb{C}^{m \times L}$ denotes noisy k-space measurements collected at $t = 1, \dots, L$ temporal frames after each excitation. The MRF image is a complex-valued matrix X of spatio-temporal resolution $n \times L$ i.e. n spatial voxels and L tem-

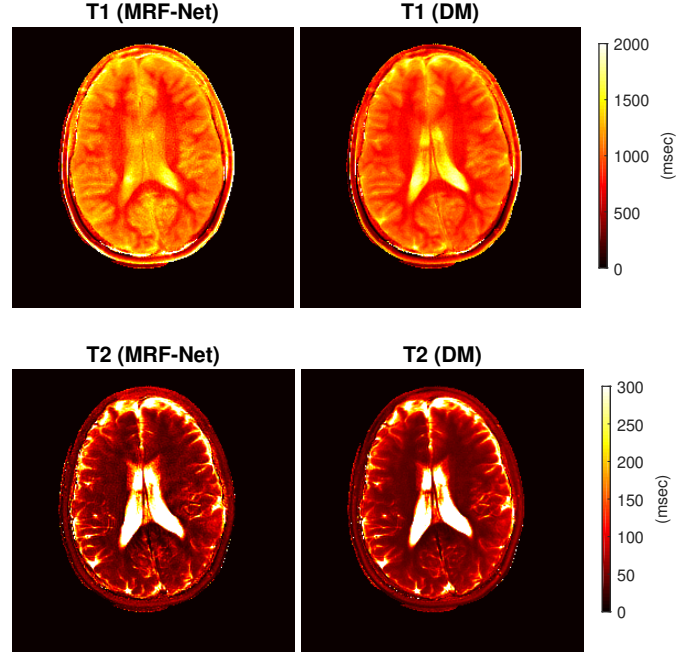


Figure 1: Reconstructed T1 and T2 maps using the proposed MRF-Net and dictionary matching (DM) baseline.

poral frames. The forward operator $\mathcal{A} := P_{\Omega}FS(\cdot)$ models multi-coil sensitivity maps S and a sub-sampled Fourier operator $P_{\Omega}F$ which represents the k-space acquisition with respect to a set of *temporally-varying* locations $\Omega = \bigcup_{t=1}^L \Omega_t$ where $\text{Card}(\Omega_t) = m \ll n$.

The main source of quantitative measurements are the per-voxel magnetization of proton dipoles obtained from dynamic rotations of the external magnetic field i.e. a sequence of Flip Angles (FA) $\{\alpha_t\}_{t=1}^L$ applying at certain repetition times $\{TR_t\}$. *Tissues with different NMR characteristics respond distinctively to these excitations.* The MRF framework relies on this principle to regularize the under-determined problem (1) by a temporal model and enable parameter estimation.

Magnetization trajectories (responses) —denoted by $\mathcal{B}(\Theta; TR, \alpha) \in \mathbb{C}^L$ —are distinct solutions of the *Bloch differential equations* for a given set of intrinsic NMR parameters $\Theta \in \mathbb{R}^p$ and excitation sequence $\{\alpha_t, TR_t\}$ [7]. Current MRF approaches discretize through a dense sampling the parameter space $[\Theta] = [T1] \times [T2] \times \dots$ and simulate a large dictionary of normalized fingerprints $D = \{D_j\}_{j=1}^d$ where,

$$D_j := \mathcal{B}([\Theta_j]; TR, \alpha) \quad \forall j = 1, \dots, d, \quad (2)$$

for all d combinations of the quantized parameters. Under the *voxel purity* assumption each spatial voxel of the MRF image corresponds to a unique NMR parameter and would approximately match to a temporal trajectory in the fingerprint dictionary: $X_v \in D \quad \forall v = 1, \dots, n$, where X_v denotes the normalized v -th row of X i.e. a multi-dimensional spatial voxel.

3 Parameter estimation

A popular approach for parameter estimation is to perform back-projection (adjoint operator) on the k-space data $\widehat{X} := \mathcal{A}^H(Y) \in \mathbb{C}^{n \times L}$ followed by dictionary matching to identify the highest correlated atom and its corresponding NMR parameters for each (normalized) voxel of the highly aliased back-projected image \widehat{X} :

$$[\Theta_v] = \text{NNS}_D(\widehat{X}_v), \quad \forall v = 1, \dots, n. \quad (3)$$

Here $\text{NNS}_D(x) := \text{argmin}_j \|x - D_j\|_2$ denotes the nearest neighbour search which serves as a Euclidean projection onto the discrete set of fingerprints i.e. manifold of Bloch Eq solutions. A temporal compression can be used to shrink the search dimension i.e. $\widetilde{X}_v := V_s^H \widehat{X}_v, \widetilde{D}_j := V_s^H D_j$ across the $s \leq L$ dominant SVD components of $DD^H \approx V_s \Lambda V_s^H$ [8]. However, enumerating the multi-parametric MRF manifold in order for (3) to be an accurate projection introduces an exponentially growing complexity (in terms of p) to the storage and computations needed for conducting NNS. A recent line of research [9, 10] shows that certain tree search strategies can benefit from the low *intrinsic dimensionality* of the MRF manifold and significantly accelerate the matching step. However storage of the dictionary or the corresponding tree still remains a big challenge for fine-grid enumerations.

3.1 MRF-Net

In this study we propose to learn a continuous map $\mathcal{F} : \mathbb{C}^s \rightarrow \mathbb{R}^p$ which approximates the MRF manifold projection:

$$\Theta_v = \mathcal{F}(\widetilde{X}_v), \quad (4)$$

where $\mathcal{F}(x) \approx \text{argmin}_{\Theta} \|x - V_s^H \mathcal{B}(\Theta)\|_2$. We train a 3-layer fully connected deep network dubbed as the MRF-Net for implementing \mathcal{F} . Similar architectures are provably shown to be efficient for manifold embedding tasks in terms of both memory and computations (see e.g. [11]). Fine-grid manifold enumeration i.e. the MRF dictionary is only used for training and not during reconstruction. MRF-Net is a feed-forward neural network which has 1 input layer and 3 hidden layers (see Figure 2b) of size 10-200-30-2. The number of outputs and the size of hidden units are customized here for a FISP MRF sequence [2] which encodes two NMR characteristics i.e. $\Theta = \{T1, T2\}$ relaxation times. MRF-Net is fed with dimension-reduced and normalized back-projected images $\widetilde{X} \in \mathbb{C}^{s \times n}$. The MRF dictionary corresponding to a FISP sequence can be represented by very few principal components [8] e.g. here $s = 10$. Thanks to this dimensionality-reduction the proposed MRF-Net requires far less units and training time as those used for the L -300-300-2 architecture proposed by [12] for solving a similar problem. To avoid losing discrimination between fingerprints we process complex-valued images as opposed to the magnitude-only data treatment used in [12].

We can formulate the network as a combination of layers connected by non-linear activation functions:

$$h^{(i)} = f\left(W^{(i)}h^{(i-1)} + b^{(i)}\right) \quad \text{for } i = 1, 2, 3.$$

where $h^{(0)} = \widetilde{X}_v, \{W^{(i)}, b^{(i)}\}$ are the weights and biases at i -th layer and $f(\cdot)$ is an element-wise nonlinear activation function. MRF-Net uses sigmoid activation for the output and ReLu for the remaining layers. The network is firstly unsupervised pre-trained successively as three standard autoencoders (Figure 2a). The MRF-Net is consequently supervised trained by

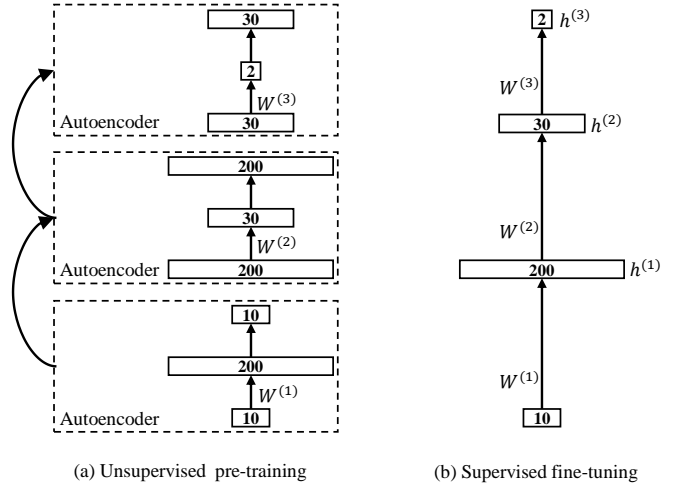


Figure 2: Illustration of the MRF-Net.

minimizing the following regression loss:

$$J(W, b) = \sum_{k=1}^3 \|h_k^{(3)} - \Theta_k\|_2^2 + \lambda \sum_{i=1}^3 \left(\|W^{(i)}\|_2^2 + \|b^{(i)}\|_2^2 \right) \quad (5)$$

where $\lambda = 10^{-5}$ controls a Tikonov regularization for stability. The normalized training inputs are dimension-reduced atoms of the fine-grid MRF dictionary \widetilde{D}_k corrupted by zero-mean independent Gaussian noises with SNRs randomly selected between 40-60 dB. After noise corruption we perform NNS searches to find correct training labels Θ_k (and not those originally generated the fingerprints) i.e.

$$h_k^3 := \mathcal{F}(\widetilde{D}_k + z_k) \quad \text{and} \quad \Theta_k := \text{NNS}_{\widetilde{D}}(\widetilde{D}_k + z_k). \quad (6)$$

We use stochastic gradient descent (SGD) to optimize (5) where the gradient updates are computed by the standard back-propagation algorithm.¹

4 In-vivo experiment

An *in-vivo* MRF dataset was acquired using the Steady State Precession (FISP) sequence in [2] and spiral readouts which sample $m = 732$ k-space locations in each of the $L = 1000$ time-frames in order to reconstruct $n = 256 \times 256$ resolution parametric maps $T1$ and $T2$.² We use the Extended Phase Graph framework [13] to simulate the Bloch responses for all combinations of $T1=[1:20:2000;2100:2000:6000]$ (ms) and $T2=[20:1:110;112:2:200;200:10:600]$ (ms), and build a dictionary with $d = 25340$ atoms for training. Fingerprints are then corrupted by adding independent Gaussian noises on-the-fly at each epoch during training. Figure 1 compares the reconstructed parametric maps using dictionary matching with brute-force searches and the proposed MRF-Net. Note that the time-memory requirement for a dimension-reduced dictionary matching —without a fast tree search—is $\mathcal{O}(snd)$ which in this example is 3x higher than requirements of the MRF-Net. This comparison is on a small-size MRF dictionary and we expect that for (emerging) applications and dictionaries encoding a large number of intrinsic parameters e.g. field inhomogeneity, perfusion, diffusion, etc, this gap substantially grows. We leave this direction for further future investigations.

¹Optimization parameters are as follows: batch size 80, 1500 epochs, momentum 0.5, drop-out factor 10^{-4} , and the step-size 10^{-2} decaying at the rate of 0.985 after every 10 iterations.

²Other scanning parameters are $TE/T_{inv}=2/18$ ms, 8 head-coils GE HDx MRI system (GE Medical Systems, Milwaukee, WI), variable density spiral sampling with 89 interleaves, 22.5x22.5cm FOV, 256 x 1mm in-plane resolution, 5mm slice thickness.

Acknowledgements

This work is partly funded by the EPSRC grant EP/M019802/1 and the ERC C-SENSE project (ERCADG-2015-694888). MG is also supported by the Scottish Research Partnership in engineering (SPRe) Award PECRE1718/18.

References

- [1] D. Ma, V. Gulani, N. Seiberlich, K. Liu, J. Sunshine, J. Durek, and M. Griswold, "Magnetic resonance fingerprinting," *Nature*, vol. 495, no. 7440, pp. 187–192, 2013.
- [2] N. Jiang Y, D. Ma, N. Seiberlich, V. Gulani, and M. Griswold, "MR fingerprinting using fast imaging with steady state precession (fisp) with spiral readout," *Magnetic resonance in medicine*, vol. 74, no. 6, pp. 1621–1631, 2015.
- [3] K. L. Wright, Y. Jiang, D. Ma, D. C. Noll, M. A. Griswold, V. Gulani, and L. Hernandez-Garcia, "Estimation of perfusion properties with mr fingerprinting arterial spin labeling," *Magnetic resonance imaging*, vol. 50, pp. 68–77, 2018.
- [4] B. Rieger, F. Zimmer, J. Zapp, S. Weingärtner, and L. R. Schad, "Magnetic resonance fingerprinting using echo-planar imaging: Joint quantification of T1 and T2* relaxation times," *Magnetic resonance in medicine*, vol. 78, no. 5, pp. 1724–1733, 2017.
- [5] C. Wang, S. Coppo, B. Mehta, N. Seiberlich, X. Yu, and M. Griswold, "Magnetic resonance fingerprinting with quadratic rf phase for simultaneous measurement of δf , T1, T2, and T2*," in *Proceedings of the Intl. Soc. Mag. Reson. Med (ISMRM)*, 2017.
- [6] M. Davies, G. Puy, P. Vandergheynst, and Y. Wiaux, "A compressed sensing framework for magnetic resonance fingerprinting," *SIAM Journal on Imaging Sciences*, vol. 7, no. 4, pp. 2623–2656, 2014.
- [7] E. Jaynes, "Matrix treatment of nuclear induction," *Physical Review*, vol. 98, no. 4, p. 1099, 1955.
- [8] D. F. McGivney, E. Pierre, D. Ma, Y. Jiang, H. Saybasili, V. Gulani, and M. A. Griswold, "SVD compression for magnetic resonance fingerprinting in the time domain," *IEEE transactions on medical imaging*, vol. 33, no. 12, pp. 2311–2322, 2014.
- [9] M. Golbabaee, Z. Chen, Y. Wiaux, and M. E. Davies, "Cover tree compressed sensing for fast MR fingerprint recovery," in *2017 IEEE 27th International Workshop on Machine Learning for Signal Processing (MLSP)*, Sept 2017, pp. 1–6.
- [10] M. Golbabaee and M. E. Davies, "Inexact gradient projection and fast data driven compressed sensing," *IEEE Transactions on Information Theory*, vol. 64, no. 10, pp. 1–15, 2018.
- [11] R. Basri and D. Jacobs, "Efficient representation of low-dimensional manifolds using deep networks," *arXiv preprint arXiv:1602.04723*, 2016.
- [12] O. Cohen, B. Zhu, and M. S. Rosen, "MR fingerprinting deep reconstruction network (DRONE)," *Magnetic resonance in medicine*, vol. 80, no. 3, pp. 885–894, 2018.
- [13] M. Weigel, "Extended phase graphs: Dephasing, RF pulses, and echoes-pure and simple," *Journal of Magnetic Resonance Imaging*, vol. 41, no. 2, pp. 266–295, 2015.